Bull. Chem. Soc. Ethiop. **2025**, 39(2), 287-300.
DOI: https://dx.doi.org/10.4314/bcse.v39i2.8

ISSN 1011-3924
Printed in Ethiopia
Online ISSN 1726-801X

SYNTHESIS, CHARACTERIZATION, ANTIOXIDANT ACTIVITY, DOCKING AND SIMULATION OF POTENTIAL ANTICANCER AGENTS OF AZO DYE FOR PYRIDYL AND ITS PALLADIUM(II) COMPLEX

Hasan Mohammed[1*], Atteqa Sultan[1], Wafa Ali Eltayb[2], Uwem O. Edet[3], Ekementeabasi Aniebo Umoh[4] and Mohnad Abdalla[5*]

[1]Chemistry Department, Science College, University of Al-Qadisiyah, Al Diwaniyah, Iraq
[2]Biotechnology Department, Faculty of Sciences and Technology, Shendi University, Shendi, Sudan
[3]Department of Biological Science (Microbiology Unit), Faculty of Natural and Applied Sciences, Arthur Jarvis University, Akpabuyo, Cross River State, Nigeria
[4]Human Physiology Department Arthur Jarvis University, Akpabuyo, Cross River State
[5]Pediatric Research Institute, Children's Hospital Affiliated to Shandong University, Jinan, Shandong 250022, People's Republic of China

(Received June 19, 2024; Revised November 1, 2024; Accepted November 4, 2024)

ABSTRACT. Herein, we describe the preparation and characterization of a novel azo dye of pyridyl, namely, (E)-N-(4-hydroxy-3-(pyridin-3-yldiazenyl)phenyl)acetamide (EHPYPA) and its palladium(II) complex. The palladium(II) complex bears the formulation [Pd(EHPYPA)Cl], which is reported by electrospray ionization mass spectrometry, CHN analysis, FT-IR, UV–Vis, ^{1}HNMR spectroscopies, molecular docking and simulation. The synthesis and structural properties of the azo dye and its palladium(II) complex are reported. The EHPYPA ligand showed important changes in the colours and spectra at different values of acidity, which permit to use of it as an indicator in analytical chemistry. The EHPYPA ligand behaves as N,O-bidentate donor ligand forming chelates. The ligand and palladium complex have been screened against the SKOV-3 cell line using the MTT method. Furthermore, the docking results indicate favourable docking with scores were -7.3 kcal/mol, -7.8 kcal/mol, and -11.2 kcal/mol for the ligand, palladium complex and Co-crystal. RMSD values for the prepared compounds indicate stability while PSA, MolSA and SASA values indicate favorable drug-like potentials for the ligands. The palladium complex has been investigated as an anticancer agent where the activity data had shown that the palladium metal complex has to be a more potent anticancer than the parent azo ligand, suggesting that metalation increases the anticancer activity of the azo ligand of pyridyl.

KEY WORDS: Cell line, Palladium, Azo, Complex, Indicator, Molecular docking

INTRODUCTION

Metal complexes are useful in many fields nowadays, especially medicinal chemistry and catalysis [1]. Cisplatin is a crucial complex of platinum ions that is frequently used as a chemotherapy medication such as testicular and ovarian malignancies. Among non-platinum anticancer medicines, palladium complexes have garnered increased interest because of their strong antiproliferative effects [2].

Azo dye containing a biotin unit used as photosensitizer (PS) under irradiation near the infrared region and absorption two-photon (TP) by photodynamic therapy (PDT) process exhibited significantly enhanced human colon tissue cancer sensitivity for PS by generating reactive oxygen species (ROS). In addition, fluorescence microscopy images revealed the ability of this PS for real-time imaging [3, 4].

Introducing heterocyclic moieties of azo dyes in drugs of antiviral, anti-cancer, and analgesics has been improved and easily tuned the bioactive properties of these drugs [5–7].

*Corresponding authors. E-mail: hasan.sh.mohemmed@qu.edu.iq, mohnadabdalla200@gmail.com

The most commercial dyes and pigments belong to are azo colorants which have a wide range of colors [8]. Azo dye ligands represent highly colored dyes and pigments, which used for dying fibers, leather, clothing, food, and dying of toys, medical devices, plastics, and cosmetics. They have important properties such as nonlinear and photo electronics, which lead to use especially in optical information storage, and biological medical studies [9–11]. The super hydrophobic properties of some azo dyes result in low-permeability paint that can be used as a water and vapour barrier to prevent the metal surfaces from corrosion [9].

Chemotherapy is one of the main treatment techniques utilized in hospitals for different cancer situations. As a result, there are many researchers developed new and improved anticancer drugs. Following the chemical design and manufacture of the compounds, a biological evaluation of the compounds in vitro cytotoxic effects occurs. A variety of methods that disclose cellular activity can be used to assess the health of cells such as the MTT method [12, 13].

Amino-pyridine is a significant molecule with several pharmacological activities and a key component for demonstrating a wide range of biological effects. The pyridyl moiety, a heterocyclic amine, has strong antibacterial and pharmacophores. Additionally, anticancer medications frequently have some drawbacks, such as unfavourable side effects, high toxicity, and inherent and acquired resistance [14]. Therefore, we prepared an azo dye of 3-aminopyridine and acetaminophen and its complex of Pd(II) to examine their physical properties involving spectral behaviours, and electrical conductance values, their efficiency against the cell lines of SKOV-3 and HdFn and molecular docking and simulation.

EXPERIMENTAL

Instrument analysis and equipment

Devices were used to complete measurements of analytical, spectroscopic, physical, magnetic, and biological properties, such as using some of them as antioxidants and anticarcinogens for the ligand and palladium complex. An electronic balance with four decimal places of the type (GMBH) from the company (Sartorius of German origin) was used to adjust the required weights of ligands, palladium chloride, and other used materials. The ultraviolet-visible spectra of the synthesized ligand and its palladium complex were measured using the UV-1650PC UV-Visible spectrophotometer. The infrared spectra (FT-IR) were recorded using a Bruker spectrophotometer within the range of (400-4000) cm^{-1} in their solid state and mixed with potassium bromide in the form of pellets. The ^{1}H-NMR proton spectra were measured using an American Bruker Spectrophotometer 500 MHz in (DMSO-d_6) as a solvent. Mass spectra were measured using the Mass AB sciex 3200 QTRAP instrument. The melting points were measured by using the instrument (Electrothermal 9300 M.P.). A Philips PW 9421 pH meter was used to measure the pH of the solutions.

The chemical materials were high purity and measured their melting points to check the purity. The 3-amino pyridine, acetaminophen, and palladium chloride were supplied from Sigma-Aldrich. Sodium hydroxide, sodium nitrite, and hydrochloric acid were supplied by the BDH company.

Preparation of (E)-N-(4-hydroxy-3-(pyridin-3-yldiazenyl)phenyl)acetamide (EHPYPA)

The EHPYPA ligand was prepared by dissolving 0.5 g (0.005 mol) of 3-aminopyridine in 15 mL of distilled water, then 4 mL of HCl (37%) was added to it and the mixture was cooled to zero degrees Celsius.

Sodium nitrite $NaNO_2$ 0.34 g (0.005 mol) was dissolved in 10 mL of distilled water, then the solution was cooled to zero degree Celsius, then add the sodium nitrite solution gradually to the

above-mentioned acid solution under cooling with stirring and keeping the temperature low, then leave it for 30 min to complete formation process of diazonium salt.

The diazonium salt solution was added drop by drop with continuous stirring to the coupling compound solution consisting of dissolving 0.8 g (0.005 mol) of acetaminophen with 15 mL of ethyl alcohol with (10 mL) sodium hydroxide aqueous (10%). The solution was left to settle for 30 min. The solution was colored, and then left overnight. The precipitate was filtered and washed several times with cold distilled water and recrystallized from an absolute ethanol solution. It was observed that a reddish-orange crystalline precipitate was formed. The precipitate was dried using a desiccator. The yield is 80% and the melting point is 205 °C. Chemical shifts of the ligand in ppm are 10.45 (s, H), 9.96 (s, H), 9.18 (s, H), 8.72(d, H), 8.36 (H), 8.00 (s, H), 7.62 (m, 2H), 7.03 (d, H), 3.41 (solvent), 2.5 (solvent), 2.02 (s, 3H) in ppm units. The elemental analysis of EHPYPA (calculated %) is C, 60.93; H, 4.72; N, 21.49, while the found (%) are C, 60.98; H, 4.77; N, 21.52.

Synthesis of palladium complex

To 15 mL solution of EHPYPA ligand 0.25 g (0.002 mol) in ethanol under stirring was added 5 mL of NaOH 0.002 g (0.002 mol). Palladium(II) chloride 0.025 g (0.0001 moles) was dissolved in 15 mL of distilled water, and then the solution of palladium chloride was acidified by adding two drops of hydrochloric acid to complete the dissolving process. The ligand solution was added to the solution of palladium chloride and the pH of the reaction mixture was justified at 9. The reaction solution was refluxed for one hour, and then the solution was left overnight. The precipitate of palladium complex was filtrated and washed several times by water. The dark brown powder complex of palladium(II) was dried, yielding, 70% and melting point of 302 °C. Chemical shifts of the palladium complex in ppm are 9.95 (H, d, J = 2), 8.87 (2H, m), 8.25 (2H, m), 7.67 (2H, m), 6.31 (H, d), 2.15 (CH_3), 2.5 (DMSO-d_6), 3.35 (D_2O residual). The elemental analysis of complex (calculated %) are C, 34.27; H, 2.43; N, 12.30, while the found are C, 34.20; H, 2.38; N, 12.41.

Preparation of the test ligands and target protein

The test of the ligands and palladium complex, and the target protein (5DSY) were prepared for docking as previously reported [15]. The ligands were sketched and their energies minimised using ChemDraw software [16]. Similarly, the protein, poly(ADP-ribose) polymerase-1 (PARP-1) was also prepared as previously reported [15]. Briefly, the native ligand attached to the protein revealed, and docking axes were revealed. Furthermore, the incomplete charges were and the prepared protein saved for further analysis.

Molecular docking (MD) and simulation (MDS)

In this study, MD and MDS were performed as previously reported [15]. MD was performed using the Allosite tool (https://mdl.shsmu.edu.cn/AST/) [17]. In the tool, the active site of the target protein was revealed. The prepared compounds were docked against the active site of the protein using the Autodock Vina tool and docking scores assigned using the London dG scoring function. The resulting docking poses were then visualised in 2D and 3D. On the other hand, MDS was performed as previously reported using the Schrodinger Desmond module [18]. In the Schrodinger Desmond module, a 140 ns simulation was carried out. To create an aqueous environment and isosmotic conditions was ensured by selecting the TIP3P model and 0.15 M NaCl. Furthermore, the boundary of the simulation box as set at 10 Å while the simulation environment was set to equilibrium (310 K and 1.013 bar).

RESULTS AND DISCUSSION

Synthesis and characterization of EHPYPA ligand and its Pd(II) complex

The 3-aminopyridine has been easily diazotized by the action of nitrous acid which was prepared from sodium nitrite and HCl at 0-5 °C to form the corresponding diazonium intermediate. In situ coupling of the freshly obtained diazonium salt with acetaminophen to furnish the coupling product, EHPYPA as shown in Scheme 1(a). The palladium(II) complex was prepared by mixing palladium chloride with EHPYPA ligand as shown in Scheme 1(b), under the equivalent ratio 1:2 metal ions : ligand.

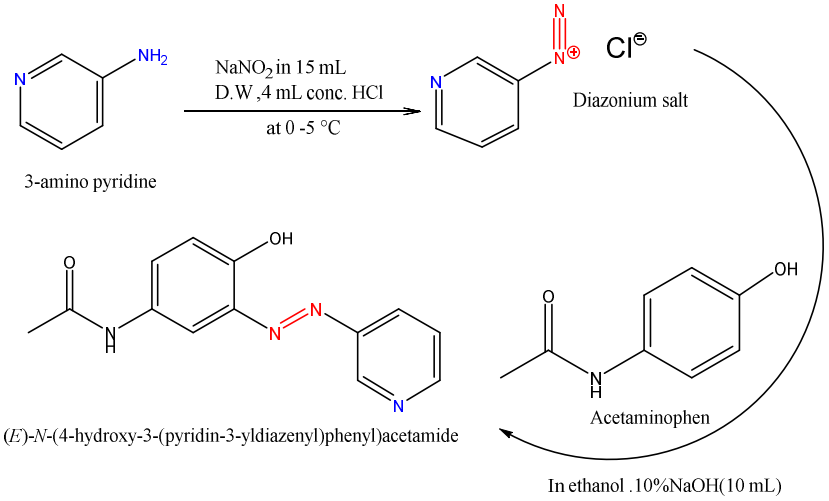

Scheme 1. (a) Preparation of (E)-N-(4-hydroxy-3-(pyridin-3-yldiazenyl)phenyl)acetamide.

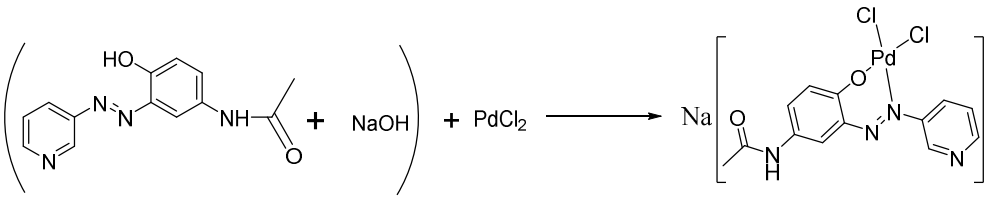

Scheme 1. (b) Preparation of pallidium complex for EHPYPA.

Preparation steps of EHPYPA ligand and its pallidum complex

The molecular structures of azo dye namely, EHPYPA of 3-aminopyridine and acetaminophen and its palladium complex were verified by a number of physico-chemical methods. The mass technique is an important method to characterise the compounds, where the EHPYPA ligand as shown in Figure 1 exhibited an important signal at 256.1 (m/z) in perfect agreement with the molecular mass of the expecting formula of EHPYPA dye ($C_{13}H_{12}N_4O_2$) and the palladium complex exhibited a signal at 430.9 m/z in agreement with the expected formula for the palladium complex ($C_{13}H_{11}N_4O_2Cl_2Pd$). The molar conductivity in DMSO solvent, which indicates the ionic properties of the complex under the ratio equal to 1:1.

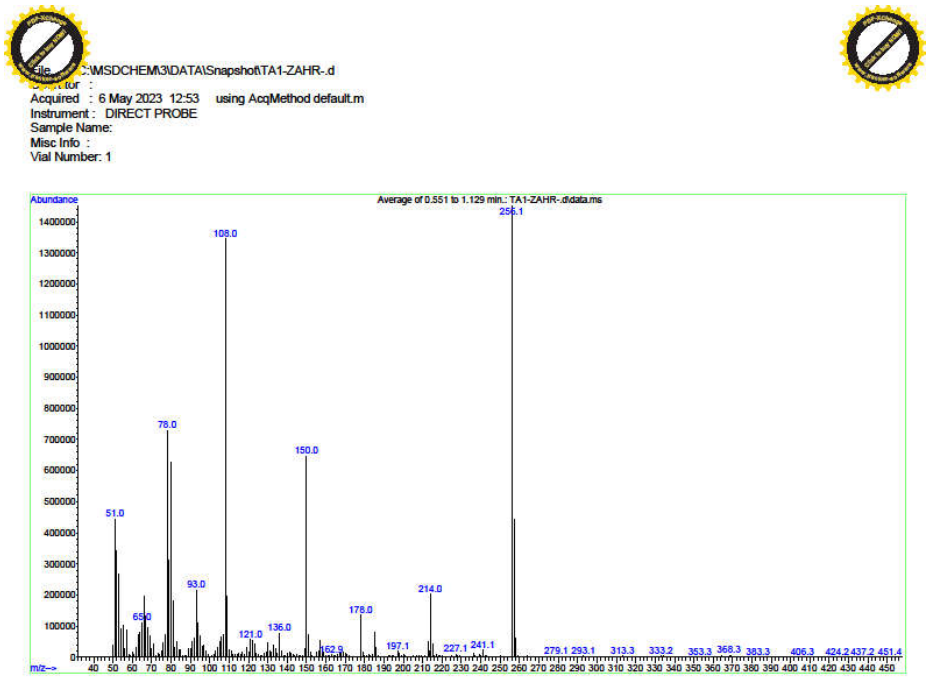

Figure 1. Mass spectrum of EHPYPA ligand.

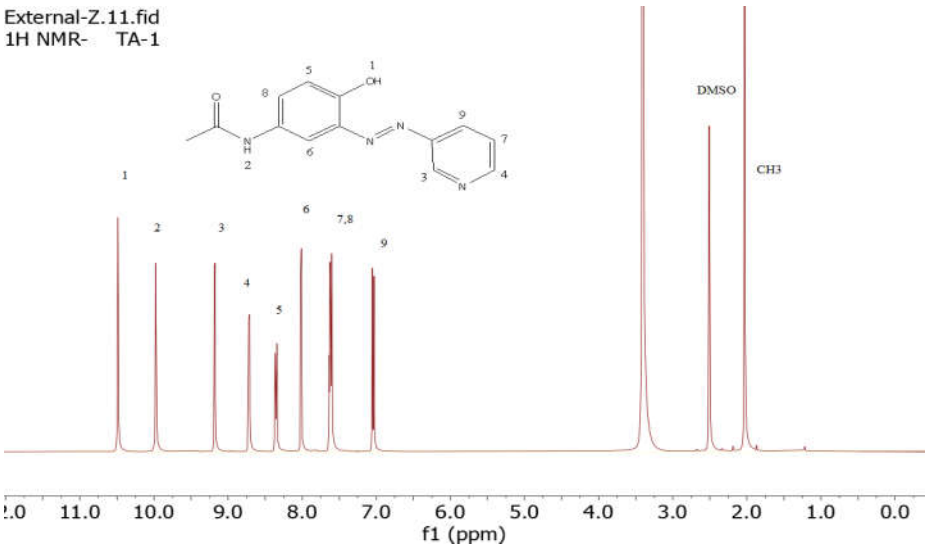

Figure 2. ^{1}H-NMR spectrum of EHPYPA ligand.

The EHPYPA ligand exhibited an interesting ^{1}H-NMR spectrum as shown in Figure 2, where indicates the number of signals with multiplicities of protons equivalents to the proposed formula of the EHPYPA ligand. The OH and NH showed in low field at 10.5 and 10 ppm as singlet signals. The CH=N moiety of pyridyl showed at 9.25 ppm as a singlet signal in the low field because there is a deshielding effect. The protons of CH_3 group showed at 2 ppm, as a single signal. The residual water and DMSO showed at 3.45 and 2.5 ppm, respectively. The signal of OH disappeared in the case of the palladium complex and there are changes in the chemical shifts of the complex protons with multiplicity equal to the number of complex protons.

Infrared spectra

The infrared spectra of the bidentate ligand and its palladium complex were recorded in the KBr pellets and the spectrum of the Pd(II) complex is compared with the free ligand to determine the coordination sites that may be involved in chelation. A comparison of the infrared spectra of the free ligand and azo complex of palladium gives us the proof of the complexation of the ligand to palladium ion. The characteristic vibration band at 3420 cm^{-1} is due to the OH group of the EHPYPA ligand which disappeared in the infrared spectrum of the complex. That means that the coordination has occurred with the oxygen atom under deportation with palladium.

The infrared spectrum of the azo ligand showed characteristic bands for aromatic N-H, C–H, aliphatic C–H, C=O, C=N, -N=N- and C–O vibrations which are listed in Table 1. The ligand showed a broad absorption band due to O–H stretching vibrations at 3420 cm^{-1}, which is probably related to the hydrogen-bonded O–H stretch. This stretch was absent in the palladium complex in agreement with the proposed structure. The absence of this band confirmed the formation of the complex by deprotonation of the phenolic group of the ligand. Upon complexation, the N=N stretching vibrations shifted from 1500 cm^{-1} to the lower frequency about 19 cm^{-1}. This shift was due to the donation of electron density from the ligand to the metal center. The ligand and its palladium complex exhibit bands at 3071-3066 and 2983-2840 cm^{-1} that are assignable to vibrations of aromatic C–H and aliphatic C–H stretching. New vibration bands, which are not present in the spectrum of the ligand appeared around 541-480 cm^{-1}, corresponding to M–O and M–N vibrations supporting the involvement of N and O atoms in coordination with the metal center [19].

Table 1. The important frequencies of EHPYPA ligand and its palladium complex.

	OH	NH	CH	CH	C=O C=N	C=C	-N=N-	M-O	M-N
EHPYPA ligand	3430	3283	3071	2930	1642	1558	1500	-	-
Pd complex		3283	3066	2950	1662	1580	1481	541	480

Electronic spectra

Absorption spectra of EHPYPA ligand and palladium complex were observed in DMSO solvent. For the EHPYPA ligand, two absorption bands appeared at 261 and 328 nm due to $\pi \rightarrow \pi^*$, and a band at 426 nm was observed which is due to $n \rightarrow \pi^*$ [20, 21]. The palladium complex exhibited a new band at 235 nm due to intra ligand. The bands of the EHPYPA ligand shifted to a higher wavelength in the spectrum of palladium complex, which were observed at 271 and 342 nm, respectively. The d-d electronic transitions of palladium complex were observed at 493, 527 and 580 nm, which are due to $^1A_{1g} \rightarrow {}^1E_{1g}$, $^1A_{1g} \rightarrow {}^1B_{1g}$ and $^1A_{1g} \rightarrow {}^1A_{2g}$, respectively, in agreement with the square configuration of Pd(II) complexes [22, 23].

pH effect on the properties of EHPYPA ligand

The absorption spectra of 10^{-4} M of EHPYPA ligand were scanned at different pH levels between 200 and 800 nm, and three distinct bands are shown for EHPYPA ligand in the vicinity of 260 and 350 nm due to $\pi \rightarrow \pi^*$ and band at 450 nm due to $n \rightarrow \pi^*$. This study clarifies the species that might arise in solutions with various pH values. At pH = 7, the EHPYPA ligand showed azo form and hydrazine form while under an acidity medium, the ligand exhibited hydrazine form and protonation in the NH group which leads to a decrease the absorption. At basic conditions, the EHPYPA ligand exhibited azo form and deprotonation of the OH group which leads to more absorption [24–27], which is in agreement with the azo group that is p-acidic which is responsible for photochromism, pH-responsive, and exhibits redox activity to ligands involving azo group [28].

Solvatochromic effect on the properties of EHPYPA dye

The UV-Vis spectra of EHPYPA ligand in different solvents such as ethanol, methanol, and dimethyl sulfoxide. There is an increasing bathochromic from ethanol to dimethylsulfoxide in agreement with the increasing of dipole moment and dielectric properties from ethanol to DMSO. The π^* of EHPYPA ligand is high polarity, therefore the increasing of the dipole moment and dielectric properties of the solvent leads to more bathochromic shift [29–32].

Cytotoxicity evaluation

The EHPYPA dye and its palladium complex are emerging as key types of medicinal compounds having an enormous potential for biological activities such as anticancer and antioxidant [33–36], therefore our objective aimed to evaluate the potential of the novel synthesized compounds for inhibiting the proliferation of human cell lines attached to ovarian cancer (SKOV-3) and health cell line of HdFn. The azo dye of acetaminophen and its palladium complex showed high anticancer potential by using MTT assay in cancer cell lines. The azo ligand displayed high excellent activity against SKOV-3 and its palladium complex showed high activity against SKOV-3 cell lines. The palladium complex was highly toxic toward SKOV-3 cancer cells with IC_{50} values of 47.78 µg/mL and was more efficient than the EHPYPA ligand, which exhibited IC_{50} values of 233.3 µg/mL. Both compounds of EHPYPA and palladium complex exhibited low cytotoxicity towards the health cell line of HdFn which was 89.9 and 301.8 µg/mL, respectively.

The DPPH assay

The ability of the compounds as antioxidants is vital for life and they can inhibition the activity of free radicals formed during the oxidation process which leads to protect the living cells from harm and abnormal metabolism [37, 38]. The DPPH method is used to show the scavenging activity of the EHPYPA ligand and palladium complex. The antioxidant results of the synthesized compounds were examined at concentrations of 12.5, 25, 50, 100, and 200 µg/mL. The scavenging activity showed clearly concentration dependent. The azo ligand (EHPYPA) exhibited excellent activity. Which may be due to the presence of OH groups in the ligand, which enhances the antioxidant nature. The complex exhibited important antioxidant activity but was lower than the azo ligand. The results of the EHPYPA ligand are too close to the results of ascorbic acid in all concentrations. The palladium result was moderate compared to the ascorbic acid and the results of palladium complex were not so much depending on the concentration.

Docking and molecular simulation result

The docking scores indicates that scores were -7.3, -7.8 and -11.2 for the ligand, palladium complex and Co-crystal. The scores indicates favorable binding for the study prepared compounds even though their scores were lower than those of the control co-crystal. The amino acids utilized in the docking for palladium complex were HIS415, ARG431 and TRY460 with individual scores that ranged from -2.7 to -4.1 kcal/mol. For the ligand, the amino acids were GLU545, GLY416, MET443, and GLU545 with scores that ranged from -1.3 to -17.2 kcal/mol. The co-crystal returned the highest number of interacting amino acids and these were GLU416, GLU545, GLY424, GLY429, SER457, HIS425 and ARG431 with scores that ranged from -0.8 to -6.6 kcal/mol. The most abundance interaction was H-acceptor bonds followed by H-donors while the least was ionic bonds.

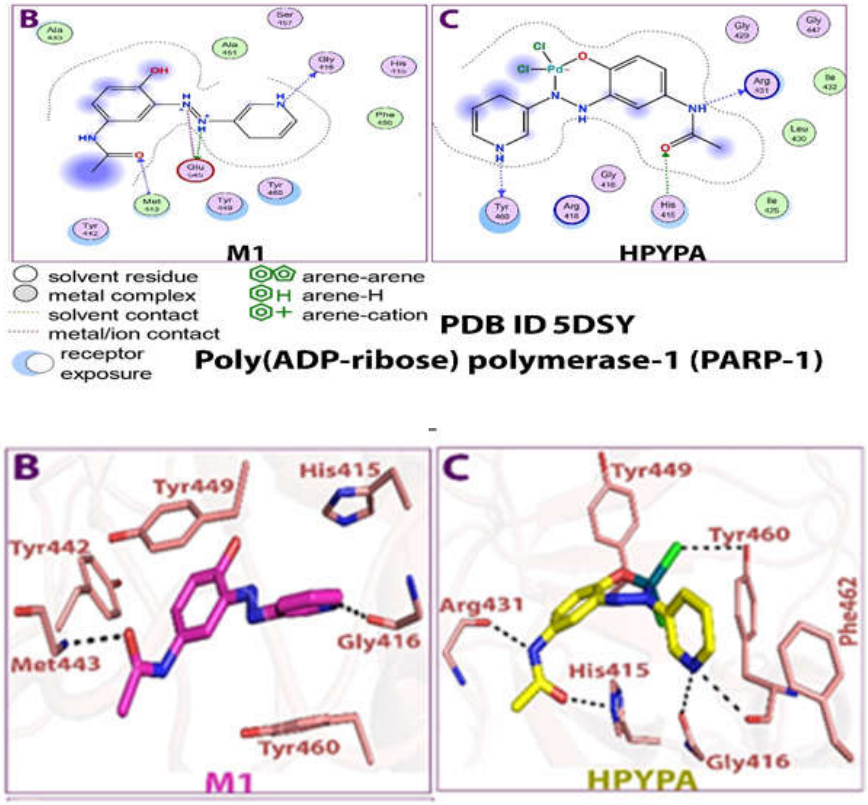

Figure 3. Molecular docking result for the various prepared compounds in 2D (Upper half)) and 3D (lower half). Key: 5DSY = Poly(ADP-ribose) polymerase-1 (PARP-1); M1 = (E)-N-(4-hydroxy-3-(pyridin-3-yldiazenyl)phenyl) acetamide; M2 = palladium complex = HPYPA.

Figure 3 shows the result of the molecular docking that was carried out between the ligands in 2D and 3D. The 2D and 3D structures reveal the various amino acids involved in the interactions. The co-crystal had more amino acids interacting with it than the test prepared compounds on the whole. Figure 3 (3D) further shows the structures of the target protein (D and E).

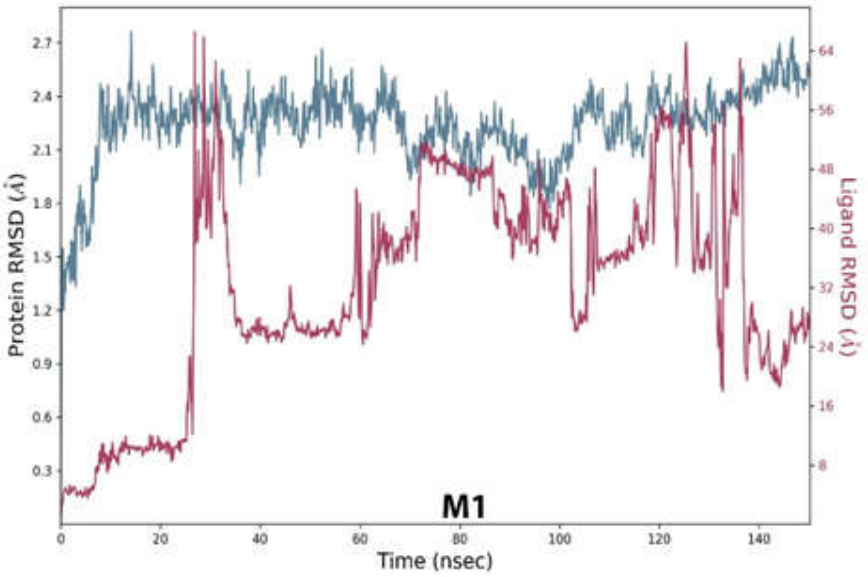

Figure 4. RMSD (140 ns) fluctuations of the various complexes formed.

Figure 4 shows the various RMSD fluctuations and as can be seen from the RMSD values, there were fluctuations across the 140 ns run. Consistently the highest RMSD value was 2.7Å for both ligands and the target protein. The ligands were generally stable (less than 2 Å) than the target protein for the first 100 ns even though there were spikes above 2 Å. Generally RMSD values less than 2 Å denote stability [15], implying that the complexes were most stable at the first 20 ns.

Figure 5 shows the RMSF values of ligand (M1) and palladium complex (M2), and the control. Consistently, all the prepared compounds showed three spikes that were above 2 Å at various amino acid residues. For the control co-crystal, the regions were at amino acid residues 60, 125 and 225 while for the ligand, the regions were 25, 120, 190 and 225 while for palladium complex, these were at 25, 120 and 145, respectively. The stable regions below 2 Å, indicates stability [15].

Protein-ligand contacts analysis for the ligand and palladium complex as well as the co-crystals indicated that the amino acids in contact with the co-crystals and the prepared compounds were 31, 98 and 70, respectively. In addition, the various bonding types for the various amino acids utilised in the bonds formed. The dominant bond types were water bridges, hydrogen and hydrophobic bonds. The dominance of these bond collectively indicate stability of the complexes especially within the vicinity of the active site of the target site [39, 40]. Furthermore, the presence of numerous water bridges indicate the readiness of the amino acids to act as donors of hydrogen [40].

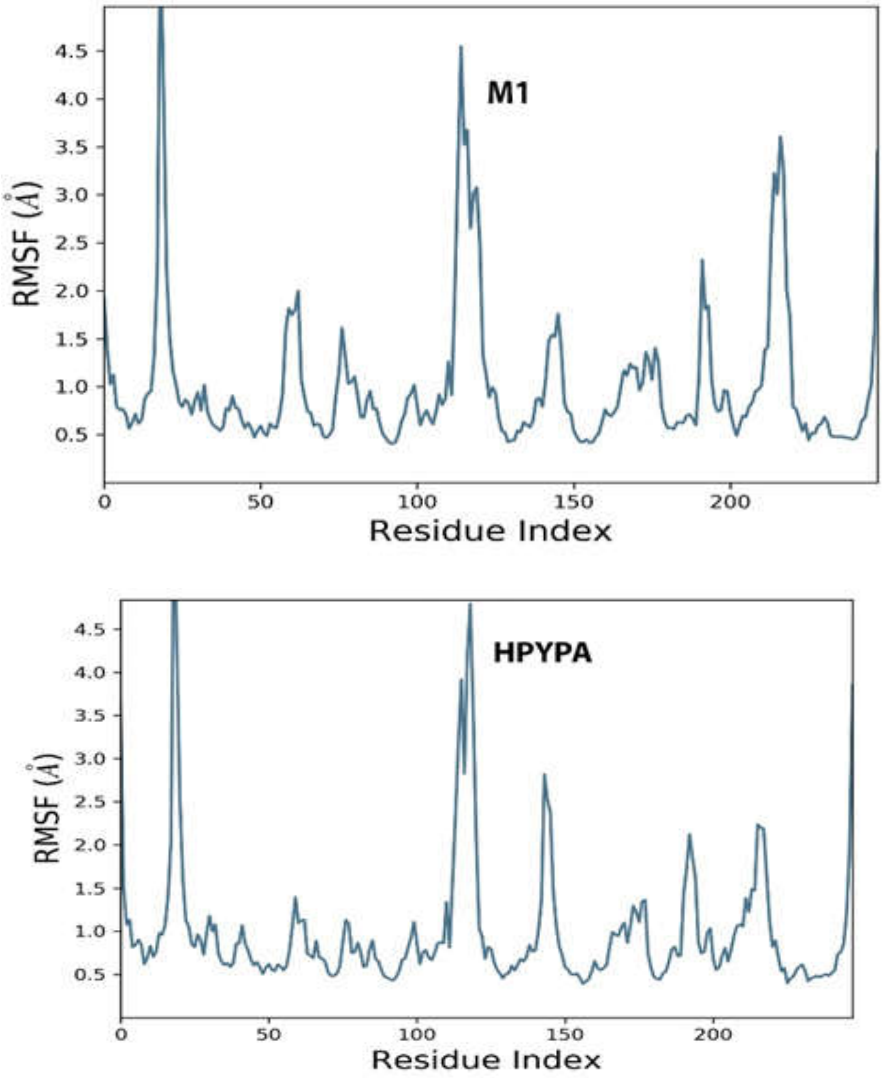

Figure 5. RMSF values of the ligand (M1), palladium complex (M2) and the control co-crystal.

For the control co-crystal, the RMSD valves ranged from 0.8 to 1.8 Å but for the ligand (M1). The range was from 0.5 to 1.5 and 0.6 to 1.8 Å for palladium complex (M2) (Figure 6). The low RMSD values for the prepared compounds indicate to the stability [15]. The rGyr values were 5.16 to 6.0, 3.75 to 4.20 and 3.30 to 3.75 Å, respectively, for the control, the ligand (M1) and palladium complex (M2). The MolSA values ranged from 460 to 490, 260 270 and 300 to 310 Å. The SASA and PSA values ranged from 50 to 200, 150 to 450, and 100 to 600; and 300 to 340, 138 to 150 and 100 to 120 Å, respectively. The RMSD returned values that were stable, that is, less than 2Å [15]. The rGyr values were less than the control values and this indicate that the ligands were more compact than the control [41]. The lower MolSA values of the ligands

compared to the control further indicates that they are capable of forming more stable complexes than the control [42]. The SASA values of the control were lower than those of the ligand (M1) and palladium complex (M2) while the PSA values of M1 and M2 were lower than that of the control. SASA and MolSA provide an indication of the increased solubility of a compound [43].

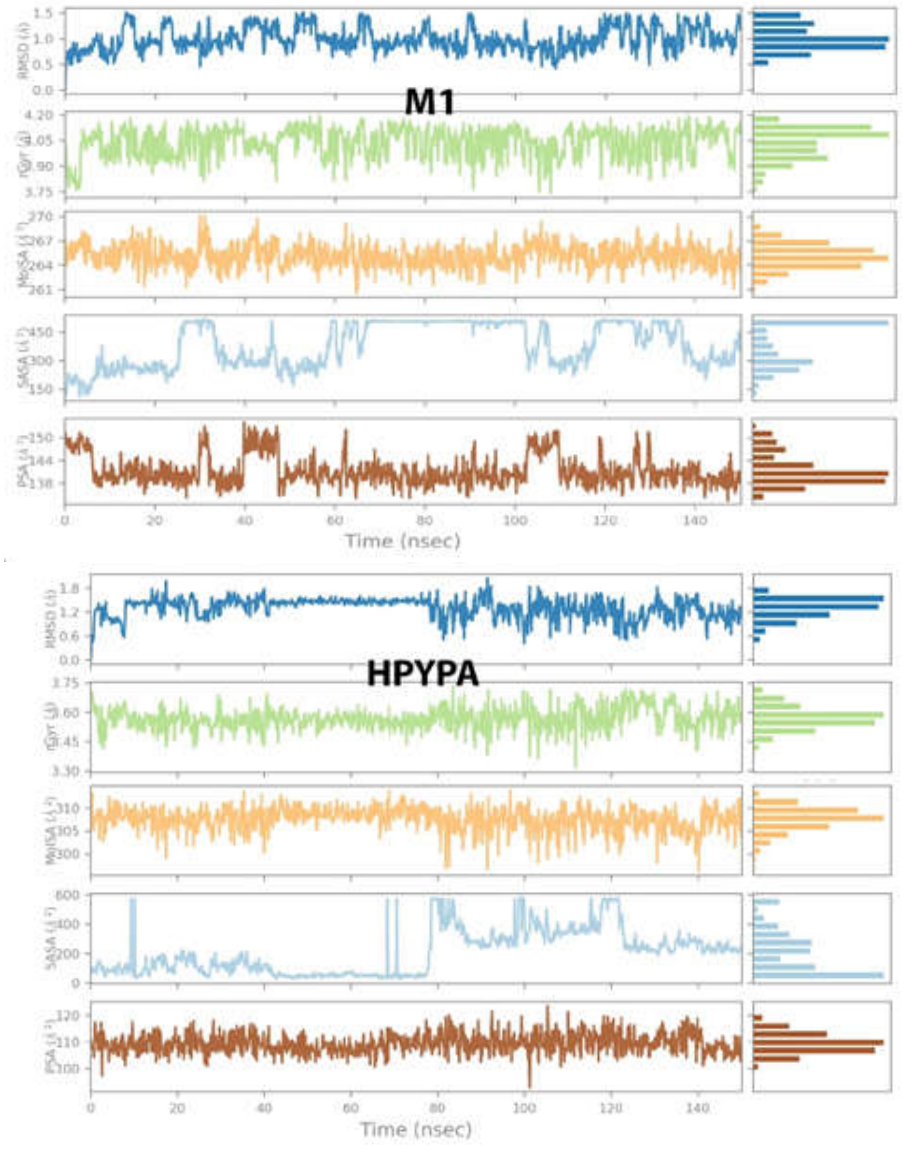

Figure 6. The ligand (M1) and palladium complex (HPYPA) interaction properties analysis.

CONCLUSION

We described in this study the synthesis, characterization, antioxidant, and anti-ovarian cancer of azo dye ligand from 3-aminopyridne (HPYPA) and its palladium complex. The compounds showed capable of inhibiting tumor cell growth and inducing cell death. The compounds were found to be nontoxic to the human normal cell line. The antioxidant activity was carried out to investigate the potential of the synthesized compounds using DPPH assay. The compounds demonstrated strong antioxidant activities, whereas the EHPYPA ligand showed strong antioxidant activity in comparison with ascorbic acid. Furthermore, docking and simulation studies indicate stable prepared compounds and favourable drug-like potentials. The presence of pyridyl, acetaminophen, and azo moieties in the synthesized compounds are important to add valuable applications as colourful materials, pharmaceutical agents, and analytical indicators. The EHPYPA ligand is bidentate and the palladium complex is square planer and ionic.

REFERENCES

1. Haribabu, J.; Srividya, S.; Mahendiran, D.; Gayathri, D.; Venkatramu, V.; Bhuvanesh, N.; Karvembu, R. Synthesis of palladium(II) complexes via Michael addition: Antiproliferative effects through ROS-mediated mitochondrial apoptosis and docking with SARS-CoV-2. *Inorg. Chem.* **2020**, 59, 17109-17120.
2. Augello, G.; Azzolina, A.; Rossi, F.; Prencipe, F.; Mangiatordi, F.; Saviano, M.; Ronga, L.; Cervello, M.; Tesauro, D. New insights into the behavior of NHC-gold complexes in cancer cells. *Pharm.* **2023**, 15, 466.
3. Mohammed, H.; Sultan, A. Synthesis and characterization of potential antioxidant agent of novel pyridylazo ligand and its palladium complex. *Bull. Chem. Soc. Ethiop.* **2024**, 38, 1301-1310.
4. Mandal, P.; Pratihar, L. A review of the photochromic behavior of metal complexes embedded in conjugated (–N= N–C= N–) and non-conjugated azo-imine-based ligands. *Rev. Inorg. Chem.* **2023**, 39, 1-10.
5. Mezgebe, K.; Mulugeta, E. Synthesis and pharmacological activities of azo dye derivatives incorporating heterocyclic scaffolds: A review. *RSC Adv.* **2022**, 12, 25932-25946.
6. Alghuwainem, A.; Abd El-Lateef, M.; Khalaf, M.; Abdelhamid, A.; Alfarsi, A.; Gouda, M.; Abdelbaset, M.; Abdou, A. Synthesis, structural, DFT, antibacterial, antifungal, anti-inflammatory, and molecular docking analysis of new VO(II), Fe(III), Mn(II), Zn(II), and Ag(I) complexes based on 4-((2-hydroxy-1-naphthyl)azo) benzenesulfonamide. *J. Mol. Liq.* **2023**, 369, 120936.
7. Frota, F.; Lorentino, A.; Barbosa, F.; Ramos, S.; Barcellos, C.; Giovanini, L.; Souza, P.; Oliveira, C.; Abosede, O.; Ogunlaja, S.; Pereira, M.; Branquinha, H.; Santos, S. Antifungal potential of the new copper(II)-theophylline/1,10-phenanthroline complex against drug-resistant Candida species. *BioMetals* **2023**, 37, 321-336.
8. Porobić, S.; Božić, B.; Dramićanin, M.; Vitnik, V.; Vitnik, Ž.; Marinović, M.; Mijin, D. Absorption and fluorescence spectral properties of azo dyes based on 3-amido-6-hydroxy-4-methyl-2-pyridone: Solvent and substituent effects. *Dyes Pigm.* **2020**, 175, 108139.
9. Mohammed, H.; Al-Hasan, H.; Chaieb, Z.; Zizi, Z.; Abed, H. Synthesis, characterization, DFT calculations and biological evaluation of azo dye ligand containing 1,3-dimethylxanthine and its Co(II), Cu(II) and Zn(II) complexes. *Bull. Chem. Soc. Ethiop.* **2023**, 37, 347-356.
10. Abdou, A.; Mostafa, M.; Abdel-Mawgoud, M. Seven metal-based bi-dentate NO azocoumarine complexes: Synthesis, physicochemical properties, DFT calculations, drug-likeness, in vitro antimicrobial screening and molecular docking analysis. *Inorg. Chim. Acta* **2022**, 539, 121043.

11. Ali, R.; Mohammed, S. Biological activity and latent fingerprints detection by azo quinoline dye and its complexes. *Period. Eng. Nat. Sci*. **2021**, 9, 317-29.
12. Ganot, N.; Meker, S.; Reytman, L.; Tzubery, A.; Tshuva, Y. Anticancer metal complexes: Synthesis and cytotoxicity evaluation by the MTT assay. *J. Vis. Exp.* **2013**, 81, e50767.
13. Petkov, N.; Pantcheva, I., Ivanova, A.; Stoyanova, R., Kukeva, R.; Alexandrova, R.; Abudalleh, A.; Dorkov, P. Novel cerium(IV) coordination compounds of monensin and salinomycin. *Molecules* **2023**, 28, 4676-4697.
14. Mallikarjuna, M.; Keshavayya, J. Synthesis, spectroscopic characterization and pharmacological studies on novel sulfamethaxazole based azo dyes. *J. King Saud Univ.-Sci.* **2020**, 32, 251-259.
15. Nwaokorie, F.; Abdalla, M.; Edet, O.; Abdalla, M.; Okpo, A.; Shami, A.; Bassey, U.; Tayeb, J.; Charlie, E.; David, O. In-silico assessment of bioactive compounds from chewing stick (*Salvadora persica*) against N-acetylneuraminate lyase (5ZKA) of *Fusobacterium nucleatum* involved in salicyclic acid metabolism. *J. Mol. Struct.* **2024**, 1316, 138733.
16. Mendelsohn, D. ChemDraw 8 Ultra, Windows and Macintosh Versions. *J. Chem. Inf. Comput. Sci.* **2024**, 44, 2225-2226.
17. https://mdl.shsmu.edu.cn/AST/).
18. Kubra, B.; Badshah, L.; Faisal, S.; Sharaf, M.; Emwas, H.; Jaremko, M.; Abdalla, M. Inhibition of the predicted allosteric site of the SARS-CoV-2 main protease through flavonoids. *J. Biomol. Struct. Dyn.* **2023**, 41, 9103-9120.
19. Fayyadh, B.; Abd, N.; Sarhan, B. Synthesis and characterization of new Mn(II), Co(II), Cd(II) and Hg(II) complexes with ligand [N-(pyrimidin-2-ylcarbamothioyl) benzamide] and their anti-bacterial study. *Earth Environ. Sci.* **2022**, 1029, 012030.
20. Alghuwainem, A.; El-Lateefm, M.; Khalaf, M.; Amer, A.; Abdelhamid, A.; Alzharani, A.; Alfarsi, A.; Shaaban, S.; Gouda, M.; Abdou, A. Synthesis, DFT, biological and molecular docking analysis of novel manganese(II), iron(III), cobalt(II), nickel(II), and copper(II) chelate complexes ligated by 1-(4-nitrophenylazo)-2-naphthol. *Int. J. Mol. Sci.* **2022**, 23, 15614.
21. Abd El-Lateef, M.; Khalaf, M.; Amer, A.; Kandeel, M.; Abdelhamid, A.; Abdou, A. Synthesis, characterization, antimicrobial, density functional theory, and molecular docking studies of novel Mn(II), Fe(III), and Cr(III) complexes incorporating 4-(2-hydroxyphenyl azo)-1-naphthol (Az). *ACS Omega* **2023**, 8, 25877-25891.
22. Emam, M.; Bondock, S.; Aldaloa, M. Schiff base coordination compounds including thiosemicarbazide derivative and 4-benzoyl-1,3-diphenyl-5-pyrazolone: Synthesis, structural spectral characterization and biological activity. *Results Chem.* **2023**, 5, 100725-100746.
23. Hamza, S.; Mahmmoud, A.; Al-Hamdani, A.; Ahmed, D.; Allaf, W.; Al Zoubi, W. Synthesis, characterization, and bioactivity of several metal complexes of (4-amino-N-(5-methyl-isaxazol-3-yl)-benzenesulfonamide). *Inorg. Chem. Commun.* **2022**, 144, 109776.
24. Chen, C.; Tao, T.; Wang, G.; Peng, X.; Huang, W.; Qian, F. Azo-hydrazone tautomerism observed from UV-vis spectra by pH control and metal-ion complexation for two heterocyclic disperse yellow dyes. *Dalton Trans.* **2012**, 41, 11107-11115.
25. Mohammed, H.; Al-Hassan H.; Abdul-Hassan, W.; Abed, H. Synthesis, characterization and biological activity of some complexes for azo dye containing 1,3-dimethylxanthine. *AIP Conference Proceedings* **2023**, 2845, 020025.
26. Mohammed, H. Synthesis and characterization of some complexes of azo-chalcone ligand and assessment of their biological activity. *Mater. Plast.* **2021**, 58, 23-31.
27. Ali, R.; Mohammed, H. Synthesis and characterization and biological study of pyridylazo ligand and its compounds of Co, Ni and Cu divalent ions. *J. Phys. Conf. Ser.* **2021**, 1999, 012009.
28. Mondal, T.; Mathur, T.; Slawin, A.; Woollins, J. Sinha, C. Imidazole-imidazolidine. Preparation by reduction of [Os (H)(CO)(PPh_3)$_2$ (PyaiR)]+/0 with $NaBH_4$ and characterisation

of the products (PyaiR = 1-alkyl-2-{3′-(pyridylazo)} imidazole). *J. Organomet. Chem.* **2007**, 692, 1472-1481.
29. Avcı, D.; Tamer, O.; Atalay, Y. Solvatochromic effect on UV–Vis absorption and fluorescence emission spectra, second- and third-order nonlinear optical properties of dicyanovinyl-substituted thienylpyrroles: DFT and TDDFT study. *J. Mol. Liq.* **2016**, 220, 495-503.
30. Mohammed, H. Synthesis, identification, and biological study for some complexes of azo dye having theophylline. *Sci. World J.* **2021**, 2021, 1-9.
31. Mohammed, H. Synthesis, characterization, structure determination from powder X-ray diffraction data, and biological activity of azo dye of 3-aminopyridine and its complexes of Ni(II) and Cu(II). *Bull. Chem. Soc. Ethiop.* **2020**, 34, 523-532.
32. Al-Krboly, M.; Sarhan, B.; Alany, A. Synthesis and characterization of new metals complexes of [N-(4-chlorobenzoylamino)-thioxomethyl] valine (cbv). *J. Appl. Chem.* **2014**, 7, 67-73.
33. Abdel-Latif, E.; Keshk, E.; Khalil, A.; Saeed, A.; Metwally, H. Synthesis, characterization, and anticancer activity (MCF-7) of some acetanilide-based heterocycles. *J. Heterocycl. Chem*. **2018**, 55, 2334-2341.
34. Sahar, Y.; Mohammed, H. Synthesis, characterization of metal complexes with azo ligand containing indole ring and study of palladium complex activity against leukemia Arab. *J. Sci. Eng.* **2023**, 1-9.
35. Sahar, Y.; Mohammed, H.; Al-Abady, Z. Synthesis and characterization of new metal complexes containing azo-indole moiety and anti-leukemia human (HL-60) study of its palladium(II) complex. *Results Chem.* **2023**, 5, 100847.
36. Sandhu, Q.; Pervaiz, M.; Majid, A.; Younas, U.; Saeed, Z.; Ashraf, A.; Khan, R.; Ullah, S.; Ali, F.; Jelani, S. Schiff base metal complexes as anti-inflammatory agents. *J. Coord. Chem.* **2023**, 76, 1094-1118.
37. Vinodkumar, J.; Pushpavathi, I., Keerthikumar, T., Maliyappa, R.; Ravi, N. Synthesis, characterization, computational and biological studies of nitrothiazole incorporated heterocyclic azo dyes. *Struct. Chem.* **2020**, 31, 1317-1329.
38. Unnisa, A.; Abouzied, S.; Baratam, A.; Lakshmi, C.; Hussain, T.; Kunduru, D.; Banu, H.; Fatima, B., Hussian, A.; Selvarajan, K. Design, synthesis, characterization, computational study and in-vitro antioxidant and anti-inflammatory activities of few novel 6-aryl substituted pyrimidine azo dyes. *Arab. J. Chem.* **2020**, 13, 8638-8649.
39. Patil, R.; Das, S.; Stanley, A.; Yadav, L.; Sudhakar, A.; Varma, K. Optimized hydrophobic interactions and hydrogen bonding at the target-ligand interface leads the pathways of drug-designing. *PloS One* **2010**, 5, 1-10.
40. Zhu, C.; Li, G.; Xiao, K.; Shao, X.; Cheng, J.; Li, Z. Water bridges are essential to neonicotinoids: Insights from synthesis, bioassay and molecular modelling studies. *Chin. Chem. Lett.* **2019**, 30, 255-258.
41. Rampogu, S.; Lee, G.; Park, S.; Lee, W.; Kim, M. Molecular docking and molecular dynamics simulations discover curcumin analogue as a plausible dual inhibitor for SARS-CoV-2. *Int. J. Mol. Sci.* **2022**, 23, 1-20.
42. Ferdausi, N.; Islam, S.; Rimti, H.; Quayum, T.; Arshad M.; Ibnat, A.; Islam, T.; Arefin, A.; Ema, T.; Biswas, P. Point-specific interactions of isovitexin with the neighboring amino acid residues of the hACE2 receptor as a targeted therapeutic agent in suppressing the SARS-CoV-2 influx mechanism. *J. Adv. Vet. Anim. Res.* **2022**, 9, 230-240.
43. Durham, E.; Dorr, B.; Woetzel, N.; Staritzbichler, R.; Meiler, J. Solvent accessible surface area approximations for rapid and accurate protein structure prediction. *J. Mol. Model.* **2009**, 15, 1093-1108.